ATLAS NOTE

July 20, 2010

J/ψ Performance of the ATLAS Inner Detector

The ATLAS Collaboration

ATLAS-CONF-2010-078
28 July 2010

Abstract

A performance study of $J/\psi \to \mu^+\mu^-$ decays is presented from 7 TeV proton-proton collisions using the ATLAS detector at the LHC with an integrated luminosity of 78 nb^{-1}. The J/ψ mass was extracted from the reconstructed di-muon invariant mass spectrum using track parameters determined from the ATLAS Inner Detector. The agreement with the PDG value of the reconstructed J/ψ mass is within statistical uncertainties and provides a validation of the momentum scale determination in the low mass region. The mass resolution is compatible with Monte Carlo expectations. The kinematic properties of the J/ψ candidates are presented and compared with Monte Carlo predictions. The reconstructed J/ψ mass and mass resolution are compared in different detector regions.

1 Introduction

The study of the J/ψ resonance with early data at the Large Hadron Collider (LHC) [1] at CERN is one of the first goals of the physics programme of the ATLAS experiment [2]. Measuring the J/ψ production cross-sections will provide sensitive tests of QCD predictions in proton-proton collisions at the LHC. Mastering the J/ψ production and properties in ATLAS is a crucial step both for understanding the detector performance and for performing measurements of various B-physics channels at the LHC.

The J/ψ resonance provides an excellent testing ground for studies of the ATLAS Inner Detector in the region of low transverse momentum (below 20 GeV) and therefore the aim of this study is to understand the behaviour of the J/ψ at very low p_{T} using the reconstructed mass and mass resolution of the J/ψ resonance. This study is part of a programme on momentum scale determination in the low mass region and is complementary to a previous study [3] using decays of the K_S particle.

This note presents studies on the J/ψ resonance in the di-muon decay channel $J/\psi \to \mu^+\mu^-$ with the ATLAS detector as of July 2010. Data collected in proton-proton collisions at centre-of-mass energy $\sqrt{s} = 7$ TeV at the LHC between the end of March and early July 2010 were used, corresponding to an integrated luminosity of 78 nb^{-1}. This work closely follows the methodology used in the first observation [4] of the J/ψ resonance by the ATLAS experiment, but exploits increased integrated luminosity and improved Inner Detector alignment and reconstruction.

Section 2 provides a brief overview of the ATLAS detector and trigger used for the current analysis. Sections 3 and 4 describe the data and Monte Carlo samples used in this study. Section 5 discusses the J/ψ candidate selection and Section 6 explains the reconstruction of J/ψ candidates and the procedure used in the J/ψ mass fit. Section 7 shows the mass fits for the whole detector and in various pseudo-rapidity regions and Section 8 describes some selected kinematic distributions of the J/ψ candidates. Section 9 shows the reconstructed invariant mass and mass resolution of the J/ψ as a function of the pseudo-rapidity of the J/ψ and its muons.

2 The ATLAS detector

The ATLAS detector is designed to fully exploit the discovery potential of the LHC. It covers almost the full solid angle around the collision point with layers of tracking detectors, calorimeters and muon chambers. For the measurements presented in this paper the trigger system, the Inner Detector (ID) tracking devices and the Muon Spectrometer (MS) are of particular importance. The coordinate system used here is described in reference [5].

The ATLAS Inner Detector [6] has full azimuthal angle ϕ coverage and spans the pseudo-rapidity range $|\eta| < 2.5$. It consists of a silicon Pixel Detector (Pixel), a silicon strip detector (SCT) and a Transition Radiation Tracker (TRT). These detectors cover a sensitive radial distance from the interaction point of 50.5 mm up to 1066 mm and are immersed in a 2 Tesla axial magnetic field. The Inner Detector barrel (end-cap) parts consist of 3 (2×3) Pixel layers, 4 (2×9) double layers of single-sided silicon strip sensors, and 73 (2×160) layers of TRT straws.

The ATLAS Muon Spectrometer [5] is designed to detect muons over a large region of pseudo-rapidity $|\eta| < 2.7$ and consists of a large toroidal magnet (with an average magnetic field of 0.5 Tesla) and four detectors, each using a different technology. Monitored Drift Tube chambers (MDT) in both barrel ($|\eta| < 1.05$) and end-cap ($1.05 < |\eta| < 2.7$) regions and Cathode Strip Chambers (CSC) in the end-caps are used as precision measurement chambers, whereas Resistive Plate Chambers (RPC) in the barrel and Thin Gap Chambers (TGC) in the end-caps are used as trigger chambers. The chambers are arranged in three layers, such that high-p_{T} particles traverse at least three stations with a lever arm of several metres.

The ATLAS detector has a three-level trigger system: Level 1 (L1), Level 2 (L2), and the Event

Filter (EF). For the measurements presented here, two different trigger chains were used. One relies on the Minimum Bias Trigger Scintillators (MBTS) while the other uses the RPC and TGC muon chambers.

The MBTS are mounted at each end of the detector in front of the Liquid Argon end-cap-Calorimeter cryostats at $z = \pm 3.56$ m. They are segmented into eight sectors in azimuth and two rings in pseudorapidity ($2.09 < |\eta| < 2.82$ and $2.82 < |\eta| < 3.84$). The MBTS trigger is configured to require two hits above threshold from either side of the detector. A dedicated muon software trigger commissioning chain at the EF level is required to confirm the candidate events chosen for this study. This is initiated by the MBTS L1 trigger and searches for the presence of at least one muon track in the entire Muon Spectrometer (the so called *full scan* procedure).

The ATLAS Level 1 muon trigger is based on the RPC chambers for the barrel region ($|\eta| < 1.05$) and on the TGC chambers for the end-cap region ($1.05 < |\eta| < 2.4$) [5]. It looks for hit coincidences within different RPC or TGC detector layers inside programmed geometrical windows which define the muon p_{T} (L1 trigger roads). It then selects muons above six programmable thresholds and provides a rough estimate of their positions. For the first data-taking period the muon trigger is used in the loosest possible setup. The only constraint is the requirement of a time coincidence between measurements in two successive planes in the middle station of the muon spectrometer RPC. No geometrical constraint (no road and then no p_{T} selection) is applied, although muons must have a momentum greater than 3 GeV to reach the MS.

3 Data sample

Collision data with a centre-of-mass energy of 7 TeV, taken between March 30th 2010 and July 5th 2010, are included in this analysis. Data are included if they are taken in a period where the LHC operators had declared the beams to be stable. Additionally, data are only included if the quality is deemed to be suitable for physics analysis, on the basis of the status of the Muon Spectrometer, Inner Detector and magnet systems. Events are also required to have passed a trigger selection, as described in Section 5. Taking into account the event selection, the total integrated luminosity for the sample is calculated to be 78 nb^{-1}. The uncertainty on the luminosity measurement is estimated to be 11%.

4 Monte Carlo sample

Monte Carlo comparisons were made using a sample of pure J/ψ generated with Pythia 6.421 [7], tuned using the ATLAS MC09 tune [8] and MRST LO* [9] parton distribution functions. The sample was generated using the Pythia implementation of prompt J/ψ production sub-processes in the NRQCD Colour Octet Mechanism framework, tuned to describe Tevatron results [10]. Zero polarisation was assumed in J/ψ di-muon decays and no attempt was made to account for polarisation effects at this time. The events were simulated with Geant4 [11] and fully reconstructed with the same software as was used to process the data from the detector.

The direct J/ψ Monte Carlo samples are used to compare the shape of the reconstructed invariant mass and resolution with the data. In this sample, both muons were confirmed to originate from the J/ψ. In order to obtain the shape of the kinematic variables of the J/ψ candidates from data, the background in the signal region is subtracted using the events from the tails of the invariant mass distribution. This procedure is described in Section 8 of this note.

Background contributions are expected to originate primarily from heavy flavour decays and the in-flight decay of pions and kaons into muons. Other background contributions are fakes from the misidentification of hadrons as muons and Drell-Yan production. In the fitting procedure these components are accounted for by the background parametrisation.

5 J/ψ candidate selection

The data used in this analysis were taken during a period of LHC commissioning in which the beam intensities were increasing, and consequently the instantaneous luminosity was rising from run to run. Since the aim of this study is to understand the behaviour of the J/ψ at very low p_T, the selection criteria in this analysis were optimised to accept as many J/ψ decays as possible. The early data analysed here provides a unique opportunity to access low p_T events which will not be available during the LHC running at high instantaneous luminosities, when the triggers that are useful in low-p_T studies will either be removed or heavily pre-scaled. In order to maximise the available statistics, an event was selected for further analysis if it passed either a L1 minimum bias trigger that also required an identified muon at EF, or a muon-based L1 trigger, both as described in Section 2. The minimum bias trigger was pre-scaled according to the instantaneous luminosity and was used in order to maximise the number of candidates from data taken at low instantaneous luminosity. The muon-based trigger was not pre-scaled for the data-taking period and was selected to maximise events at higher luminosities.

Each event is required to contain at least one primary vertex built from at least three tracks, each of which containing at least one measurement in the Pixel Detector and at least six in the SCT detector. In each surviving event, all pairs of oppositely-charged reconstructed muons are formed. Only muons associated with ID tracks that have at least one hit in the Pixel Detector and six in the SCT are accepted. In order for a muon to be identified in the MS, it is required to have a total momentum of at least 3 GeV. The 3 GeV minimum total momentum requirement implies a minimum transverse momentum that varies as a function of pseudo-rapidity. In combination with a reduction in efficiency in the forward region, these effects lead to a natural minimum muon p_T of approximately 1 GeV. This effect is seen in both Monte Carlo and data. No further cut on p_T is applied to these tracks, however, a cut of $p_T > 0.1$ GeV is applied automatically to all Inner Detector tracks by the reconstruction software.

Muon identification and reconstruction extends to pseudo-rapidities of up to $|\eta| = 2.7$, covering a wide p_T range. In the muon reconstruction algorithms, three categories of muons are identified: standalone (MS) muons, tagged (ID) muons and combined (both MS and ID) muons. A tagged muon is the combination of ID tracks extrapolated to the MS, and MS measurements that are not already used to form a muon.

The track parameters of the reconstructed muon are those of the Inner Detector track, in this analysis. The muon tagging covers the pseudo-rapidity range $\eta < 2$. The analysis performed in the previous note [4] required at least one combined muon. In this study, J/ψ candidates can be formed from muon pairs in which either muon can be tagged or combined.

Contamination from cosmic-ray background may come from a pair formed by a cosmic-ray muon and a muon from the collision. This probability is estimated to be very small ($< 10^{-4}$) from the 900 GeV data analysis [12]. A cosmic-ray muon mimicking a J/ψ decaying back-to-back is excluded because muons detected in the MS can only have momentum higher than 3 GeV.

The two Inner Detector tracks from each pair of muons passing these selections are fitted to a common vertex using the ATLAS offline vertexing tools based on the Kalman filtering method [13]. No constraints on mass or pointing to the primary vertex are applied to the fit, and only a loose cut on the χ^2 of the vertex fit is applied ($\chi^2 < 200$). Those pairs that successfully form a vertex are regarded as $J/\psi \to \mu^+\mu^-$ candidates. No explicit momentum or pseudo-rapidity selection is applied to the candidates. Fewer than 2% of events have more than one J/ψ candidate in the invariant mass range 2–4 GeV and pass the final event selection. In such cases, if more than one J/ψ candidate is formed from the same muon, each J/ψ is kept. The J/ψ candidates that are not from the signal decay form part of the combinatorial background which is considered as the background component of the fit, described in Section 6.

Identical trigger and event selection were applied to Monte Carlo simulated events.

6 Fitting procedure for $J/\psi \to \mu^+\mu^-$ signal candidates

Invariant mass distributions are studied for the selected muon pairs. In all cases, ID track parameters are used to calculate the properties of the J/ψ candidates. Once the vertex fit is applied, the refitted track parameters and error matrices are used to calculate the invariant mass and the per-candidate mass error. Only the statistical uncertainties were considered in the fit.

An unbinned maximum likelihood fit was used to extract the mean reconstructed J/ψ mass and the number of J/ψ signal candidates from the data. The likelihood function L is defined by:

$$L = \prod_{i=1}^{N} \left[a_0\, f_{\mathrm{sig}}(m^i_{\mu\mu}, \delta m^i_{\mu\mu}) + (1 - a_0)\, f_{\mathrm{bkg}}(m^i_{\mu\mu}) \right], \tag{1}$$

where N is the total number of pairs of oppositely-charged muons in the invariant mass range 2 GeV $< m_{\mu\mu} <$ 4 GeV. The functions f_{sig} and f_{bkg} are probability density functions that model the J/ψ signal and background mass shapes in this range and a_0 is the fraction of di-muon pairs originating from J/ψ decays in the sample of events. For the signal, the mass is modelled with a Gaussian distribution:

$$f_{\mathrm{sig}}(m_{\mu\mu}, \delta m_{\mu\mu}) \equiv \frac{1}{\sqrt{2\pi}\, S\, \delta m_{\mu\mu}}\, e^{-\frac{(m_{\mu\mu}-m_{J/\psi})^2}{2(S\,\delta m_{\mu\mu})^2}}\,, \tag{2}$$

where the mean value $m_{J/\psi}$ is the J/ψ mass and $\delta m_{\mu\mu}$ is the measured mass error calculated for each muon pair from the covariance matrix of the vertex fit. The width is the product $S\,\delta m_{\mu\mu}$, where the scale factor, S, is a parameter of the fit that represents the difference between the actual and expected mass resolution.

The background distribution is parameterised by a first order polynomial, normalised within the invariant mass range 2–4 GeV, which is given by:

$$f_{\mathrm{bkg}}(m_{\mu\mu}) \equiv \frac{1}{2} - b\,(m_{\mu\mu} - 3)\,, \tag{3}$$

where b is a parameter of the fit.

The fit returns values of the free parameters a_0, $m_{J/\psi}$, S, b and a covariance matrix of the fit. These are used to calculate other characteristics of the data. The number of J/ψ signal decays N_{sig} and its uncertainty are calculated from a_0 and its uncertainty, and the total number of pairs N.

The mass resolution σ_m is defined as the half-width of the region of the J/ψ mass distribution for which the integral of the sum of $f_{\mathrm{sig}}(m_{\mu\mu}, \delta m_{\mu\mu})$ over all candidates retains 68.27% of N_{sig}. The uncertainty on σ_m is calculated using the covariance matrices of the fitted vertices. The number of background events N_{bkg} in the mass interval $m_{J/\psi} \pm 3\sigma_m$ and its error are calculated from a_0, N and the uncertainties of a_0, $m_{J/\psi}$ and σ_m. The same fit procedure is applied to the prompt J/ψ Monte Carlo events, in which case $f_{\mathrm{bkg}}(m_{\mu\mu}) \equiv 0$.

7 Reconstructed J/ψ mass

The invariant mass distribution for all oppositely-charged muon pairs passing the selection criteria described in Section 5 is shown in Figure 1. The J/ψ mass returned by the fit is 3.095 ± 0.001 GeV, which is consistent with the the PDG value of 3.096916 ± 0.000011 GeV [14]. The number of the J/ψ signal decays is 5350 ± 90 and the mass resolution of J/ψ signal is 71 ± 1 MeV. The number of background pairs in the mass range 2.88–3.31 GeV, corresponding to $m_{J/\psi} \pm 3\sigma_m$, is 2560 ± 60. In the same figure, the mass distribution obtained from the prompt J/ψ Monte Carlo sample, normalised to the number of signal events extracted from the fit to data, is also shown.

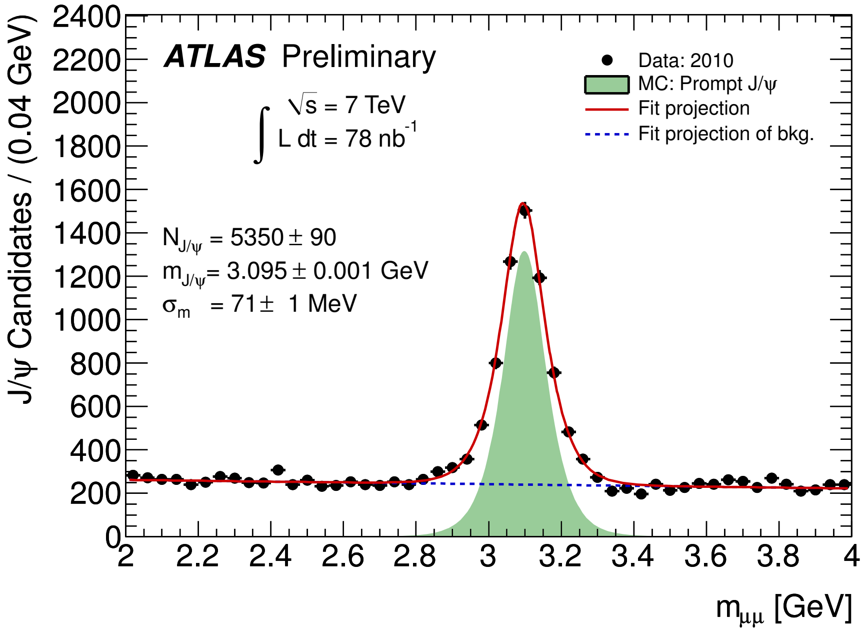

Figure 1: The invariant mass distribution of reconstructed $J/\psi \to \mu^+\mu^-$ candidates from data is shown as the black points. The solid line is the projection of the result of the unbinned maximum likelihood fit to all di-muon pairs in the mass range 2–4 GeV, the dashed line is the projection for the background component of the same fit. The filled distribution shows the prompt J/ψ Monte Carlo prediction, normalised to the number of signal events extracted from the fit to data.

The invariant mass resolution depends on the pseudo-rapidity of the two muon tracks. To illustrate this effect, all accepted J/ψ candidates are divided into three classes according to the pseudo-rapidity of the muons.

BB: Both muons in the barrel region.

EB: One muon in the end-cap and one in the barrel.

EE: Both muons in the end-cap.

The muon is labelled a barrel muon when its pseudo-rapidity is $|\eta| < 1.05$ and an end-cap muon when $1.05 < |\eta| < 2.5$. Figure 2 shows the J/ψ mass distributions for these three categories. The distributions for the prompt J/ψ Monte Carlo events are also shown, and the results of the fits are summarised in Table 1.

The mass width obtained in the fit with both muons in the end-cap region (EE) is ~2.5 times wider than that obtained from the fit with both muons in the barrel (BB). This behaviour is in part caused by the higher amount of material in the forward region of the detector and is well reproduced in the Monte Carlo. In addition to increased material traversed through the detector, at higher pseudo-rapidities the muon has a shorter effective trajectory in the magnetic field, which degrades the momentum resolution, hence impacting on the performance of the J/ψ resonance mass resolution. In all cases, the data agree with the Monte Carlo simulation and the known J/ψ mass [14] within the statistical precision available in this measurement. Furthermore, relative to the previous note [4], the agreement between data and Monte Carlo has improved with increased integrated luminosity and improved Inner Detector alignment and reconstruction.

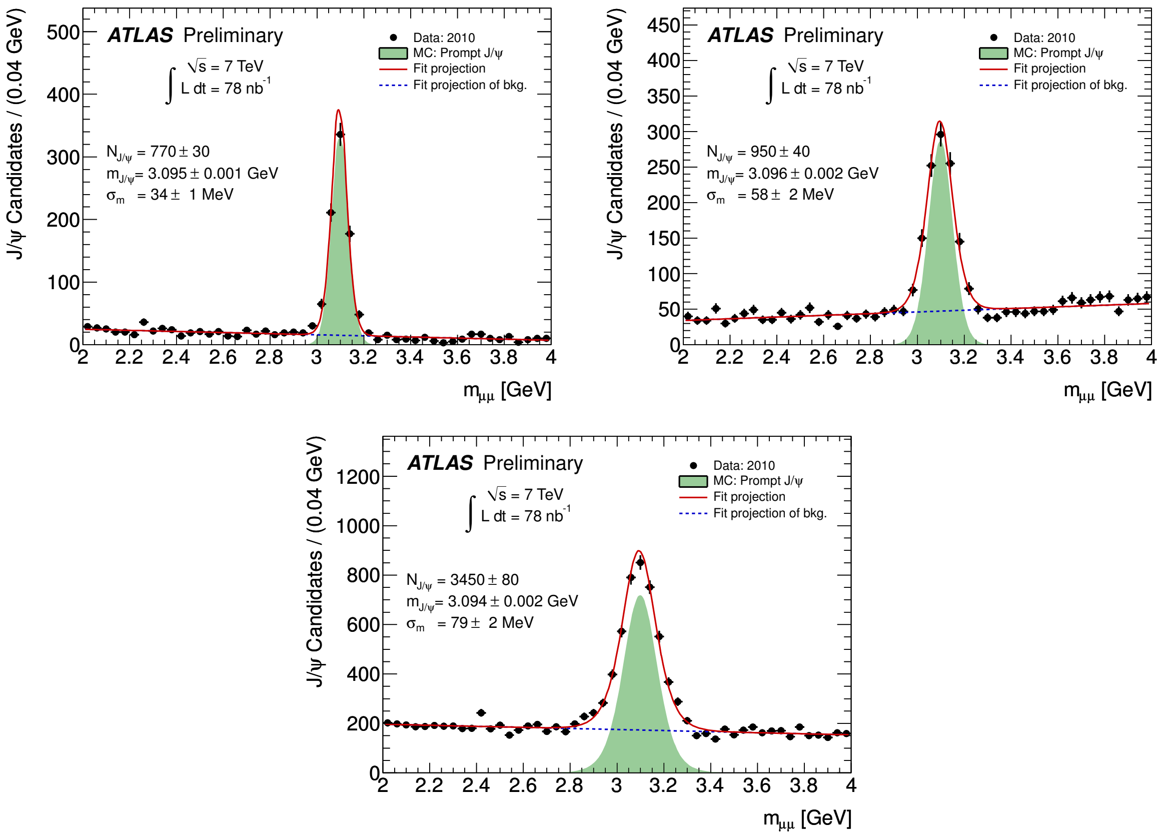

Figure 2: Invariant mass distribution of $J/\psi \to \mu^+\mu^-$ candidates in three muon pseudo-rapidity categories: both muons in the barrel (*top left*), one muon in the end-cap, one in the barrel (*top right*), both muons in the end-cap (*bottom*). The muon is labelled a barrel muon when its pseudo-rapidity is $|\eta| < 1.05$ and an end-cap muon when $1.05 < |\eta| < 2.5$. The solid lines illustrate the results of the unbinned maximum likelihood fit to all oppositely-charged di-muon pairs in the mass range 2–4 GeV. The dashed lines are the projection for the background-only component of the same fit. The filled distribution shows the prompt J/ψ Monte Carlo prediction, normalised to the number of signal events extracted from the fit to data.

Table 1: Summary of fit results to mass distributions of $J/\psi \to \mu^+\mu^-$ candidates from data and prompt J/ψ Monte Carlo. The number of background events as estimated from the fit is given in the range of $m_{J/\psi} \pm 3\sigma_m$.

	$m_{J/\psi}$ [GeV]	σ_m [MeV]	N_{sig}	N_{bkg}	S
All data	3.095 ± 0.001	71 ± 1	5350 ± 90	2560 ± 60	1.19 ± 0.02
All MC	3.0988 ± 0.0002	69.3 ± 0.2			1.133 ± 0.003
BB data	3.095 ± 0.001	34 ± 1	770 ± 30	80 ± 10	1.12 ± 0.04
BB MC	3.0983 ± 0.0004	37.0 ± 0.3			1.152 ± 0.008
EB data	3.096 ± 0.002	58 ± 2	950 ± 40	410 ± 20	1.21 ± 0.05
EB MC	3.0990 ± 0.0004	52.9 ± 0.3			1.137 ± 0.006
EE data	3.094 ± 0.002	79 ± 2	3450 ± 80	2050 ± 60	1.18 ± 0.03
EE MC	3.0989 ± 0.0003	78.5 ± 0.2			1.129 ± 0.003

8 Kinematic distributions of the J/ψ candidates

This section presents the distributions of J/ψ candidates and their muons in terms of selected kinematic quantities: transverse momentum, p_{T}; pseudo-rapidity, η; rapidity; and pseudo-rapidity of the most forward muon used to construct each J/ψ, $\eta_{\max}$.

The signal region is defined as the di-muon invariant mass range of 2.7 GeV $< m_{\mu\mu} <$ 3.5 GeV, and sideband regions for events in the ranges: 2.2 GeV $< m_{\mu\mu} <$ 2.7 GeV, and 3.5 GeV $< m_{\mu\mu} <$ 4.0 GeV. The plots in this section show the J/ψ candidates after removing the background. The shape of background contribution is estimated from the events that fall into the sidebands. This distribution is then scaled to match the background level in the signal region, as determined from the fit.

The Monte Carlo distributions are shown, normalised to the number of signal events found in data.

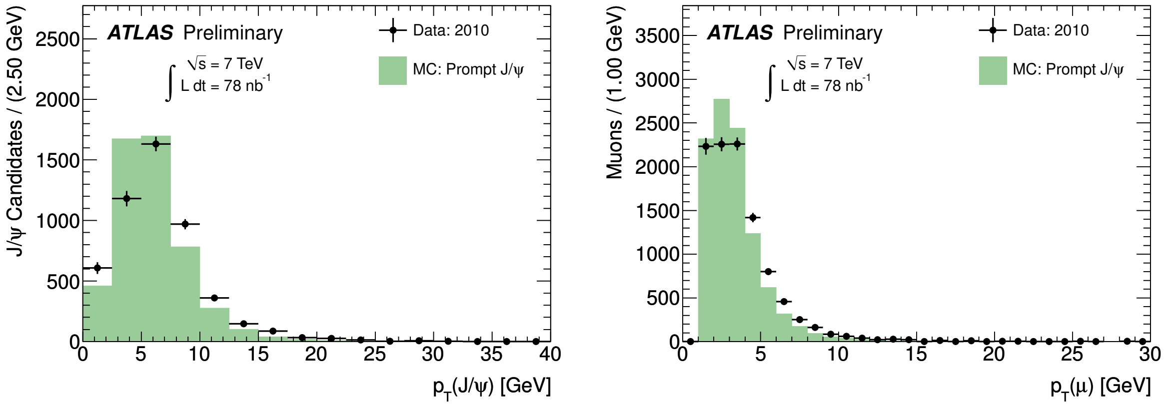

Figure 3: The transverse momentum distribution for the J/ψ candidates (*left*), and the muons used to form the J/ψ candidates (*right*). The black points correspond to events from data in the signal region of the invariant mass distribution, with the backgrounds subtracted using the tails of the invariant mass distribution. The filled area is the distribution of events from the prompt J/ψ Monte Carlo, normalised to the same number of events.

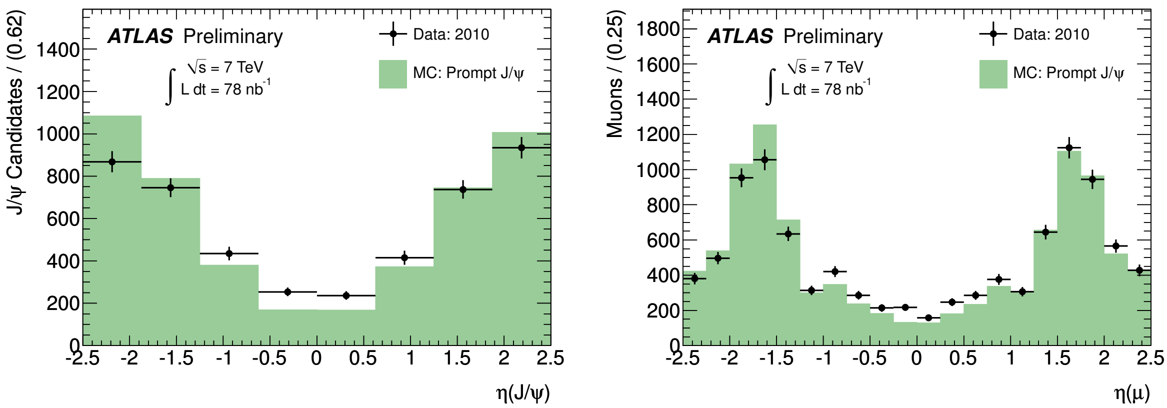

Figure 4: The pseudo-rapidity distribution for the J/ψ candidates (*left*), and the muons used to form the J/ψ candidates (*right*). The black points correspond to events from data in the signal region of the invariant mass distribution, with the backgrounds subtracted using the tails of the invariant mass distribution. The filled area is the distribution of events from the prompt J/ψ Monte Carlo, normalised to the same number of events.

The transverse momentum distribution of the observed and simulated J/ψ events are shown in Figure 3. This figure also shows the transverse momentum distributions of the muons used to reconstruct the J/ψ. As a consequence of their very low p_{T}, the J/ψ candidates have preferentially high pseudo-rapidity. The decay products of these low p_{T} J/ψ events tend to reach the Muon Spectrometer in the forward region (where $p \gg p_{\mathrm{T}}$). Figure 4 shows the pseudo-rapidity distributions for the J/ψ candidates and the muons. The rapidity of the J/ψ and the muons is shown in Figure 5. Figure 6 shows the pseudo-rapidity distribution of the muon with the higher pseudo-rapidity.

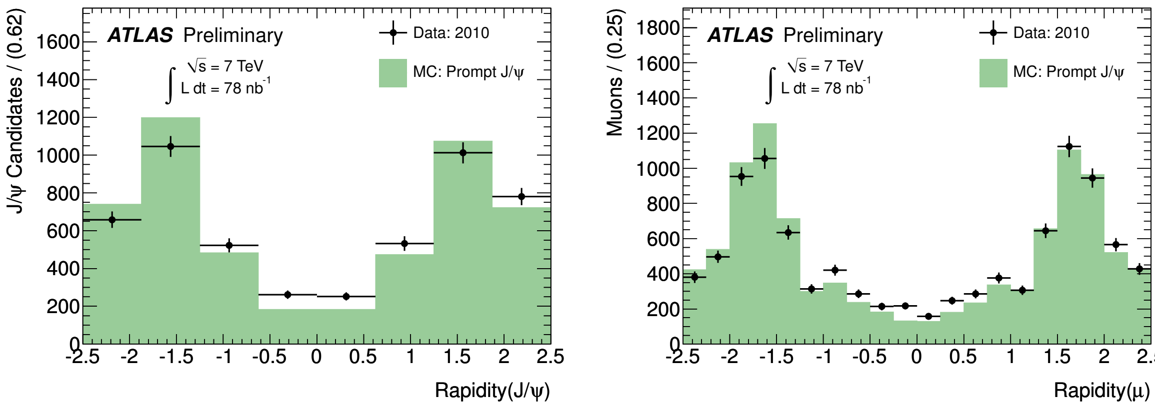

Figure 5: The rapidity distribution for the J/ψ candidates (*left*), and the muons used to form the J/ψ candidates (*right*). The black points correspond to events from data in the signal region of the invariant mass distribution, with the backgrounds subtracted using the tails of the invariant mass distribution. The filled area is the distribution of events from the prompt J/ψ Monte Carlo, normalised to the same number of events.

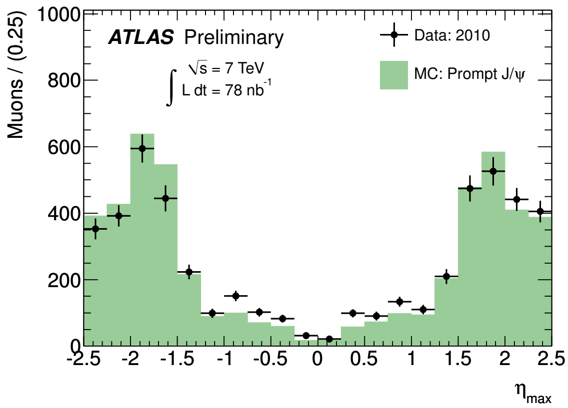

Figure 6: The pseudo-rapidity distribution of the muon with the higher pseudo-rapidity that forms the J/ψ candidate. The black points correspond to events from data in the signal region of the invariant mass distribution, with the backgrounds subtracted using the tails of the invariant mass distribution. The filled area is the distribution of events from the prompt J/ψ Monte Carlo, normalised to the same number of events.

9 Reconstructed J/ψ mass and resolution as function of kinematic observables

The reconstructed mass and mass resolution are expected to be sensitive to the level of understanding of the detector. Early J/ψ events are used in this analysis to search for possible deviations from the nominal J/ψ mass in various pseudo-rapidity regions. The mass resolution of the J/ψ is extracted from data and compared with Monte Carlo in several pseudo-rapidity regions of the detector. The pseudo-rapidity regions are defined in terms of the η of the J/ψ , and also the η of the most forward of the muons, $\eta_{\max}$, from the J/ψ candidate.

The values of the reconstructed mass and the mass resolution were determined from data using the unbinned maximum likelihood method, described in Section 6, applied over the mass range 2–4 GeV. As such, each point in the following plots is the result of a maximum likelihood fit to all the events in that kinematic range. The horizontal position of each point is weighted according to the population of the bin. The error-bars on each point along the horizontal axis of these plots illustrate the ranges from which events were selected.

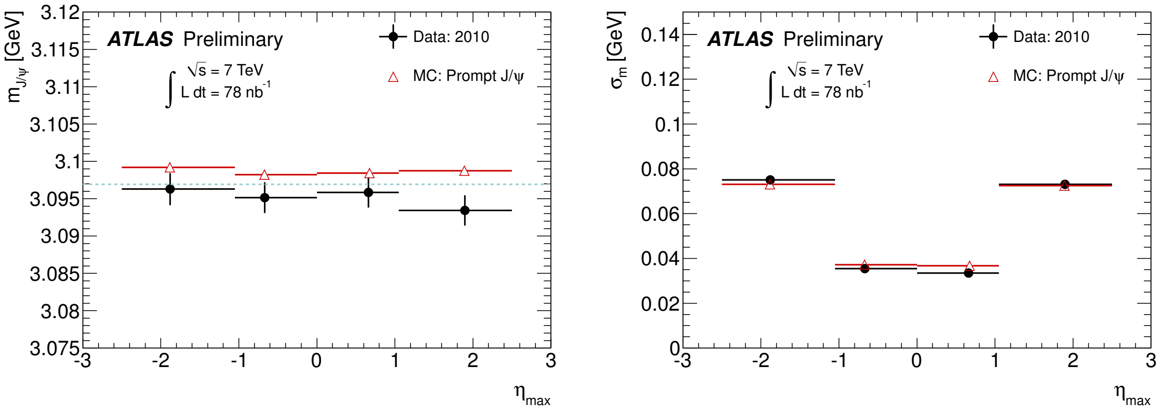

Figure 7: Reconstructed mass (*left*) and mass resolution (*right*) of the J/ψ as a function of the pseudo-rapidity of the furthest forward muon. The dashed line corresponds the PDG value of the J/ψ mass.

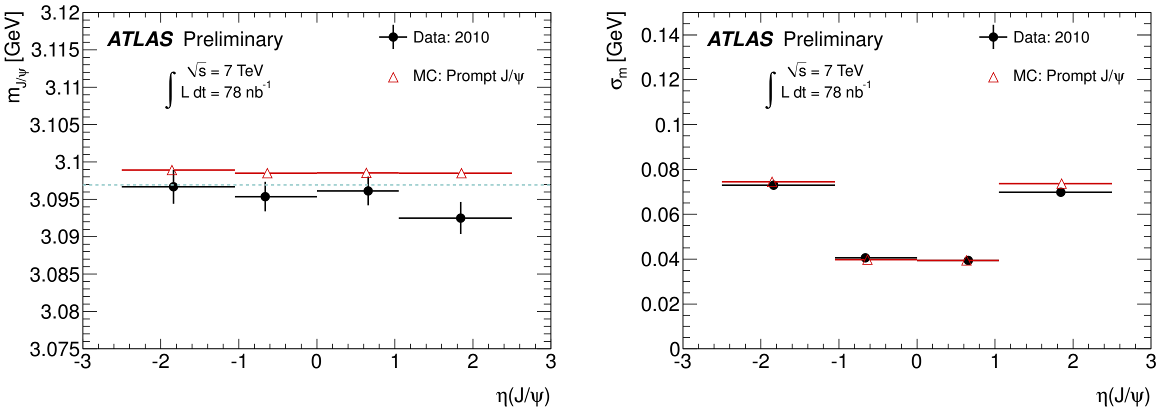

Figure 8: Reconstructed mass (*left*) and mass resolution (*right*) as a function of $\eta(J/\psi)$. The dashed line corresponds the PDG value of the J/ψ mass.

Figure 7 shows the fitted reconstructed mass and the mass resolution in four pseudo-rapidity regions. In this case, the pseudo-rapidity used was the pseudo-rapidity η_{max} of the most forward muon used to reconstruct the J/ψ. As expected, J/ψ candidates that are observed in the forward regions of the detector have a wider mass resolution than those seen in the central region.

Figure 8 shows the mass and the mass resolution as a function of the J/ψ pseudo-rapidity. The reconstructed mean masses are similar to those observed for the muon η_{max}. In both the barrel region and the end-cap region, the reconstructed data are in very good agreement with the PDG mass value. In the positive-η end-cap region ($\eta > 1.05$), the reconstructed mass is 5 MeV lower than the nominal J/ψ mass. These deviations are within the statistical errors of the test. Therefore in all of the considered η regions, there is no deviation larger than $(0.2 \pm 0.1)\%$ in the mean of the reconstructed mass. A similar level of understanding of the momentum scale at low p_{T} in the Inner Detector has been demonstrated using the reconstructed K_S mass [3]. In that case, the momentum scale is understood with a precision better than 0.1% [3].

10 Summary and conclusions

The $J/\psi \to \mu^+\mu^-$ signal has been reconstructed in ATLAS using combined information from the Muon Spectrometer and the Inner Detector. Inner Detector track parameters were used to calculate parameters of J/ψ candidates. With 78 nb^{-1} of data, the J/ψ mass peak is fitted using an unbinned maximum likelihood method and the fit yields an overall reconstructed mean mass of 3.095 ± 0.001 GeV. This is in agreement with the known PDG value for the J/ψ mass within the statistical uncertainty. The mass resolution is 71 ± 1 MeV, which is consistent with Monte Carlo expectations. The mass resolution varies with the pseudo-rapidity of the muons as expected. This variation is in agreement with Monte Carlo within statistical uncertainties. No deviations larger than (0.2 ± 0.1)% of the reconstructed J/ψ mass from its PDG value were observed in any of the pseudo-rapidity regions considered. This agreement provides a validation of the momentum scale determination at low mass region.

The kinematic properties of the J/ψ, transverse momentum and rapidity, were also studied. They were found to be in agreement with Monte Carlo within statistical uncertainties. The final number of observed $J/\psi \to \mu^+\mu^-$ candidates is 5350 ± 90. Future high statistics J/ψ samples will allow for detailed studies of the Inner Detector performance, in particular studies of the description of the material and systematic misalignments. This work will provide a solid foundation for such studies.

References

[1] L. Evans and P. Bryant, *LHC machine*, JINST **3** (2008) S08001.

[2] ATLAS Collaboration, *The ATLAS Experiment at the CERN Large Hadron Collider*, JINST **3** (2008) S08003.

[3] ATLAS Collaboration, *Study of the Material Budget in the ATLAS Inner Detector with K^0_S decays in collision data at $\sqrt{s}$=900 GeV*, ATLAS-CONF-2010-019, CERN, Geneva, Apr, 2010.

[4] ATLAS Collaboration, *First observation of the $J/\psi \to \mu^+\mu^-$ resonance in ATLAS pp collisions at $\sqrt{s}$= 7 TeV*, ATLAS-CONF-2010-045, CERN, Geneva, May, 2010.

[5] *The ATLAS Muon Spectrometer Technical Design Report detector*, CERN-LHCC-97-22, CERN, Geneva, Mar, 1997.

[6] ATLAS Collaboration, *The ATLAS Inner Detector commissioning and calibration*, arXiv:1004.5293, CERN, Geneva, Jun, 2010.

[7] T. Sjöstrand, S. Mrenna, and P. Z. Skands, *PYTHIA 6.4 Physics and Manual*, arXiv:hep-ph/0603175, May, 2006.

[8] ATLAS Collaboration, *ATLAS Monte Carlo tunes for MC09*, ATL-PHYS-PUB-2010-002, CERN, Geneva, Mar, 2010.

[9] A. Sherstnev and R. S. Thorne, *Parton Distributions for LO Generators*, arXiv:0711.2473, Nov, 2008.

[10] P. Nason et al., *Bottom production*, arXiv:hep-ph/0003142, Aug, 2001.

[11] S. Agostinelli et al., *Geant4: A simulation toolkit*, Nucl. Instrum. Meth. A **506 no. 3** (2003) 250 – 303.

[12] ATLAS Collaboration, *Charged Particle Multiplicities From p-p Interactions at $\sqrt{s}$=900 GeV measured with the ATLAS Detector at the LHC*, Phys. Lett. B **688** (2010) 21–42.

[13] V. Kostyukhin, *VKalVrt - package for vertex reconstruction in ATLAS*, ATL-PHYS-2003-031, CERN, Geneva, Aug, 2003.

[14] C. Amsler et al., *Review of Particle Physics, partial update for the 2010 edition, (Particle Data Group)*, Phys. Lett. B **667** (2008-2009) no. 1-5, 1–6.